Coincidence time resolution of 30 ps FWHM using a pair of Cherenkov-radiator-integrated MCP-PMTs

Physics in Medicine & Biology

LETTER

Coincidence time resolution of 30 ps FWHM using a pair of Cherenkov-radiator-integrated MCP-PMTs

To cite this article: R Ota *et al* 2019 *Phys. Med. Biol.* **64** 07LT01

IOP Publishing Phys. Med. Biol. 64 (2019) 07LT01 (6pp) https://doi.org/10.1088/1361-6560/ab0fce

Physics in Medicine & Biology

IPEM Institute of Physics and Engineering in Medicine

CrossMark

RECEIVED
25 January 2019

REVISED
12 March 2019

ACCEPTED FOR PUBLICATION
14 March 2019

PUBLISHED
29 March 2019

LETTER

Coincidence time resolution of 30 ps FWHM using a pair of Cherenkov-radiator-integrated MCP-PMTs

R Ota[1,2,5,6], K Nakajima[2], I Ogawa[2], Y Tamagawa[2], H Shimoi[3], M Suyama[3] and T Hasegawa[4]

[1] Central Research Laboratory, Hamamatsu Photonics K. K., Hamamatsu, Japan
[2] Faculty of Engineering, University of Fukui, Fukui, Japan
[3] Electron Tube Division, Hamamatsu Photonics K. K., Hamamatsu, Japan
[4] School of Allied Health Science, Kitasato University, Kitasato, Japan
[5] 5000, Hirakuchi, Hamakita-ku, Hamamatsu, 434-8601 Japan
[6] Author to whom any correspondence should be addressed.

E-mail: ryosuke.ota@crl.hpk.co.jp

Keywords: Cherenkov radiator, micro channel plate photomultiplier tube (MCP-PMT), coincidence time resolution (CTR)

Abstract

Radiation detectors dedicated to time-of-flight positron emission tomography (PET) have been developed, and coincidence time resolution (CTR) of sub-100 ps full width at half maximum (FWHM) has been achieved by carefully optimizing scintillators and photodetectors. Achieving a CTR of 30 ps FWHM by using a pair of annihilation γ-rays would allow us to directly localize the annihilation point within an accuracy of 4.5 mm. Such direct localization can potentially eliminate the requirement of image reconstruction processes in clinical PET systems, which would have a huge impact on clinical protocols and molecular imaging. To obtain such a high CTR, researchers have investigated the use of prompt emissions such as Cherenkov radiation and hot-intra band luminescence. Although it is still challenging to achieve a CTR of 30 ps FWHM even with a Cherenkov-based detector, the experimentally measured CTR is approaching the goal. In this work, we developed a Cherenkov-radiator-integrated micro-channel plate photomultiplier tube (CRI-MCP-PMT), where there are no optical boundaries between the radiator and photocathode, and its timing performance was investigated. By removing the optical boundaries, reflections are eliminated and transmission to the photocathode is improved, resulting in high timing capability. As a result, a CTR of 30.1 ± 2.4 ps FWHM, which is equivalent to a position resolution of 4.5 ± 0.3 mm along a line of response (LOR), was obtained by using a pair of CRI-MCP-PMTs.

1. Introduction

The coincidence time resolution (CTR) of radiation detectors for time-of-flight positron emission tomography (TOF-PET) has been improved in recent decades. The system CTRs of current clinical TOF-PET range from 200 to 600 ps full width at half maximum (FWHM) (Schung *et al* 2015, Vandenberghe *et al* 2016, Sluis *et al* 2019) and these CTRs are equivalent to a position resolution of 30–90 mm along a line of response (LOR). If the system CTR of the TOF-PET can be improved down to 30 ps FWHM, the position resolution will approach 4.5 mm along the LOR, which is of the order of the spatial (x, y) resolution of current clinical TOF-PET systems. In such a PET system with an extremely high time resolution, image reconstruction processes, which tend to amplify the noise of the PET images, are not required and the quality of each detected photon will be maximized because the TOF information can directly yield position information of positron annihilation, at the order of the spatial (x, y) resolution of the PET image. Such direct position determination will allow us to image radiotracer accumulation in a patient event-by-event, and it will allow us to get better images or similar images at shorter scan times. Thus, it is worthwhile to develop radiation detectors with a CTR of 30 ps FWHM for PET imaging.

There are two approaches to obtain a high CTR: (1) increasing the light collection efficiency (LCE), and (2) detection of Cherenkov photons. High CTR can be obtained with increase of the LCE because photon counting statistics will help improve the CTR (Cates *et al* 2015). Techniques for increasing the LCE using scintillation-based detectors have been reported (Knapitsch and Lecoq 2014, Berg *et al* 2015). Modifying the crystal surfaces selectively can increase the efficiency with which scintillation light is collected by a photo-detector and alleviate the optical mismatch between the scintillation crystal and entrance surface of the photo-detector, resulting in improvement of the energy and timing resolution. Using a low-aspect-ratio crystal is also effective to improve the LCE relative to that of a high-aspect-ratio one (Cates and Levin 2018).

CTR of sub-100 ps FWHM has been observed using a fast scintillator, such as LGSO:Ce or LSO:Ce:Ca, coupled to a silicon photomultiplier (Nemallapudi *et al* 2015, Cates and Levin 2016). In the case of a scintillation-based detector, prompt emission, including Cherenkov radiation and hot-intra band luminescence, plays an important role in improving the CTR (Lecoq *et al* 2014, Gundacker *et al* 2016, Cates and Levin 2018, Gundacker *et al* 2018). Bismuth germanate (BGO) crystal, which is widely used as the conventional scintillator for non TOF-PET scanners, showed a CTR of several hundreds of pico-seconds, based on the detection of Cherenkov photons (Kwon *et al* 2016, Brunner *et al* 2017), revealing the potential of BGO as a scintillator for TOF-PET. Detection of Cherenkov photons using semiconductor detectors coupled to silicon photomultipliers can yield sub-nano-second CTR (Ariño-Estrada *et al* 2018). Thus, the importance of detecting Cherenkov photons has been demonstrated.

In the case of a Cherenkov-based detector where the Cherenkov radiator does not emit any scintillation photons, CTR of sub-100 ps FWHM has been measured (Korpar *et al* 2011, Ota *et al* 2019). However, the number of Cherenkov photons emitted by a photoelectron with energy of several hundreds of keV is only 30 at most (Lecoq *et al* 2010, Brunner *et al* 2014, Dolenec *et al* 2016, Ota *et al* 2018). Therefore, it is necessary to effectively guide the Cherenkov photons to the photocathode of the photo-detector and increase the LCE. The Cherenkov-based detector of Korpar *et al* (2011) or Ota *et al* (2019) consists of a lead fluoride (PbF_2) as the Cherenkov radiator (refractive index 1.82 at 400 nm) coupled to a micro-channel-plate photomultiplier tube (MCP-PMT) with a magnesium fluoride (MgF_2)-based window face plate (WFP) (refractive index 1.39 at 400 nm). Therefore, optical boundaries exist between the radiator and the photo-detector, reducing the LCE. As increasing LCE can improve timing resolution (Cates *et al* 2015), one approach to improving CTR is to eliminate the optical boundaries.

In this work, we propose a detector where the optical mismatches are quite mitigated, to increase the LCE and improve the timing performance. The proposed technique is simpler than those used in the previous detectors (Knapitsch and Lecoq 2014, Berg *et al* 2015). We developed a new MCP-PMT where the Cherenkov radiator is integrated, which is referred as a Cherenkov-radiator-integrated MCP-PMT (CRI-MCP-PMT). The timing performance of the detector was experimentally investigated. Finally, we demonstrated the high CTR of the proposed detector.

2. Materials and methods

2.1. Cherenkov-radiator-integrated MCP-PMT (CRI-MCP-PMT)

The WFP of the ordinary MCP-PMT was replaced by a lead glass, which was used as a Cherenkov radiator. Owing to a large effective atomic number of the lead glass and high transparency of more than 80% in the visible region, the lead glass-based WFP is sensitive to 511 keV γ-rays and a large number of Cherenkov photons will be emitted in the lead glass. The dimensions and the active area of the lead glass were 11 mm $\phi \times 3.2$ mm and 11 mm ϕ, which are the same as those of the ordinary MgF_2-based WFP.

In the case of the ordinary MCP-PMT, a multialkali photocathode is deposited on the MgF_2-based WFP. However, direct deposition of the photocathode on the lead glass initiates a chemical reaction between them and the photocathode will be insensitive to visible light. To prevent the chemical reaction, an Al_2O_3 intermediate layer was optically stacked between the lead glass and the photocathode by using an atomic layer deposition method. The radiators with and without the intermediate layer after being exposed to alkali metals and a conceptual view of the Al_2O_3 layer are illustrated in figure 1(a). The radiator without the layer completely turned black, whereas no color change was observed for the one with it. Transmission measurements from 300 to 800 nm using a spectrophotometer (UH4150, Hitachi High-Technologies Corporation) can be also shown in figure 1(b). The intermediate layer efficaciously protects the radiator from the chemical reaction throughout the visible region. In this way, the CRI-MCP-PMT without any optical boundaries was developed.

2.2. Experiment and analysis

Figure 2 illustrates experimental setup for evaluation of the CTR. A pair of CRI-MCP-PMTs were located face-to-face and exposed to an ^{22}Na point source collimated by a 1.0 mm $\phi \times 50$ mm Pb collimator. The entrance surface of the CRI-MCP-PMT was covered by a black tape (Super 33+, 3M) to suppress reflections of the Cherenkov photons in the radiator. Signals of the CRI-MCP-PMTs were directly monitored by an oscilloscope (Keysight, DSO-404A) at 20 GS s^{-1} with a set bandwidth of 4.2 GHz. Two hundred data points per input channel were stored event-by-event. A high-voltage of -3100 V was supplied to each CRI-MCP-PMT.

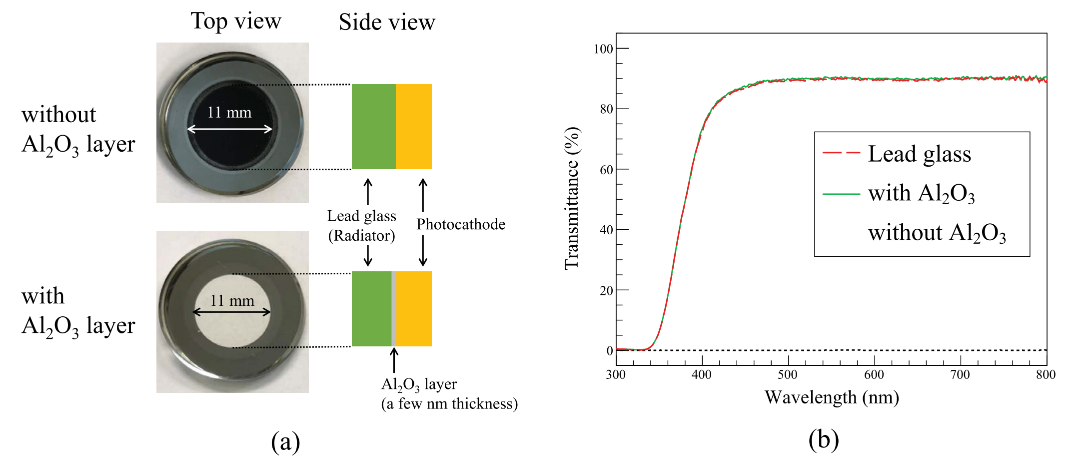

Figure 1. (a) Radiators with and without the Al_2O_3 intermediate layer after being exposed to alkali metals for the photocathode. No color change was observed for the lead glass-based WFP with the intermediate layer fabricated using atomic layer deposition technique. (b) Results of transmission measurements from 300 to 800 nm. The lead glass with Al_2O_3 intermediate layer is as transparent as the pure lead glass throughout the visible region.

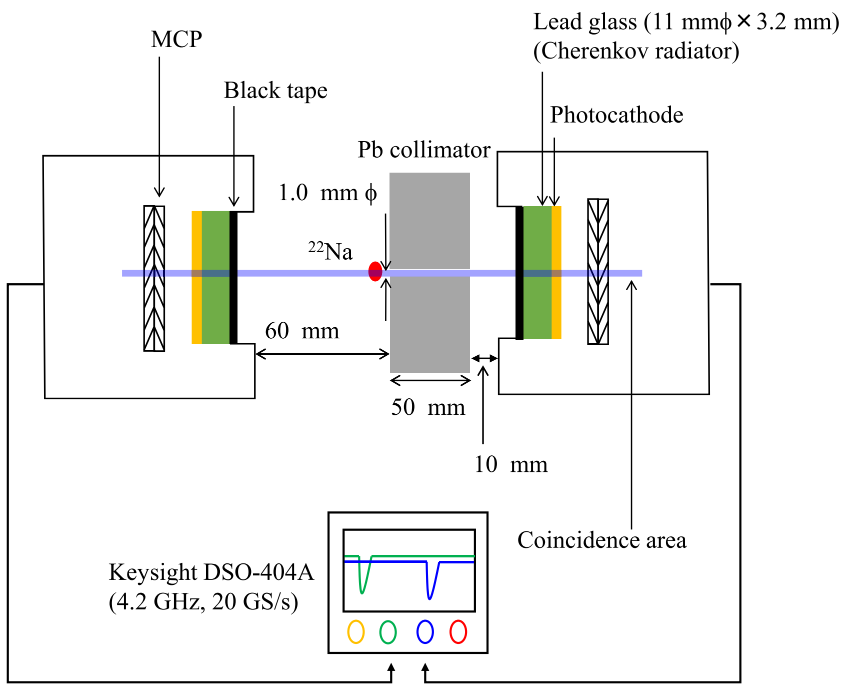

Figure 2. Experimental setups for CTR measurement. A pair of CRI-MCP-PMTs were placed face-to-face and exposed to a ^{22}Na point source using a 1.0 mm ϕ Pb collimator. The entrance surfaces of the CRI-MCP-PMTs were covered by black tapes to suppress reflections in the radiator.

The best CTR was analyzed while scanning the threshold level for timing pick-off and a pulse area window. A spline curve was obtained from the waveform data event-by-event using the TSpline3 class method in ROOT (Brun and Rademakers 1997), and detection timings at arbitrary threshold levels were numerically calculated as shown in figure 3(a). In this study, the threshold level was determined as the ratio of the pulse height and scanned from 2% to 26% to avoid time walk correction according to Ota *et al* (2019). The pulse area window was scanned with a step size of 1.25×10^{-3} V ns, and its width was set to 0.015 V ns. A histogram of the pulse area of the detector is illustrated in figure 3(b).

The CTRs were evaluated as the functions of the threshold level for timing pick-off and pulse area window. A function of 'single Gaussian + constant' was fitted to the histogram of the time difference between the two detectors, and the CTR was defined as the FWHM of the Gaussian. Throughout the fitting procedure, the fitting parameters' errors are defined as 1σ.

The total measurement time of the experiment was 2110 min, and the number of coincidence events was 20 256.

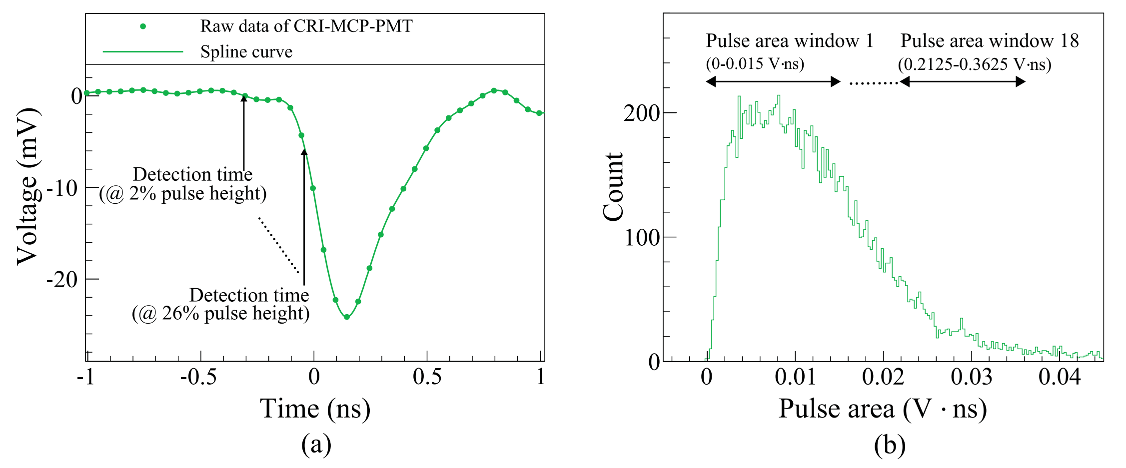

Figure 3. (a) Raw data of the CRI-MCP-PMT and the spline curve. The threshold level for timing pick-off is numerically scanned from 2% to 26% for the pulse height using the spline curve. (b) Histogram of the pulse area obtained from the CRI-MCP-PMT. The pulse area window is set to 0.015 V ns and scanned with a step size of 1.25×10^{-3} V ns.

3. Results

From the experiment, we found that the CTRs depend on the threshold levels for timing pick-off and pulse area window. The CTRs as the functions of the threshold level and pulse area are shown in figure 4(a). The pulse area region larger than 0.03 V ns could not be investigated due to the small number of coincidence events.

The best CTR is obtained with a high pulse area and low threshold level relative to the pulse height. However, the lowest threshold level does not provide the best CTR; therefore, an optimal threshold level should be used. The best CTR of 30.1 ± 2.4 ps FWHM at 5% threshold level with the pulse area window from 0.021 25 to 0.036 25 V ns was obtained, whereas the worst CTR was 48.3 ± 1.5 ps FWHM at 3% threshold level with the pulse area window from 0.001 25 to 0.016 125 V ns. The histogram of the best CTR is illustrated in the figure 4(b). The pulse area window for the best CTR contained 3.2% of the total collected events. The two side peaks around the main peak were caused by the direct detection in the MCP (Ota *et al* 2019). At a high threshold level, the CTR becomes worse once the pulse is larger than 0.025 V ns. This is because the data includes overflow events, where the threshold level for timing pick-off cannot be properly defined.

CTRs of 41.9 ± 0.6 and 34.6 ± 1.4 ps FWHM at the 5% threshold level were obtained when using all the collected events, and 15% of the collected events, respectively.

4. Discussion

The CTR of 30.1 ps FWHM, which corresponds to a position resolution of 4.5 mm along the LOR, was obtained using the pair of CRI-MCP-PMTs. Since the position resolution of 4.5 mm is of the order of the spatial (x, y) resolution of clinical PET scanners, direct position reconstruction would be feasible. This timing performance is owing to nonexistence of the optical boundaries, thinness, and the low-aspect-ratio of the radiator. According to Cates and Levin (2018), the low-aspect-ratio crystals have the potential to improve the timing performance compared to conventional high-aspect-ratio crystals like $3 \times 3 \times 20$ mm^3.

From figure 4(a), higher pulse area window provides better CTR at the optimized threshold level. Threshold optimization is required in the case of scintillation-based detectors to minimize the CTR as well (Seifert *et al* 2012, Cates *et al* 2015), where enormous number of photons are emitted and detected by a photo-detector within a nanosecond. Estimating that approximately 3 Cherenkov photons are detected in the high pulse area region (pulse area $>$ 0.02 V ns), this mitigates the single photon time resolution (SPTR) by a factor of $1/\sqrt{3}$. Since the SPTR of CRI-MCP-PMT is the same as that of R3809 MCP-PMT (25 ps FWHM (Hamamatsu Photonics K. K. 2019)), the SPTR-based timing uncertainty will be 20.4 ps FWHM ($\sqrt{2} \times 25/\sqrt{3}$). This value is almost the same as the photon-travel-spread in the radiator. According to Ota *et al* (2018), the photon-travel-spread in a PbF_2 radiator with 3.0 mm thickness is 17.0 ps FWHM. Thus, the achievable CTR will be 26.5 ($=\sqrt{20.4^2 + 17.0^2}$) ps FWHM. The difference between the experimental result and the theoretical value may be due to electrical noise and the difference in the radiator and its dimensions.

The physical factor which most strongly limits the CTR is the small number of the detected Cherenkov photons. If the number of detected photons could be increased to 10, the predicted CTR would be 20.3 ps, which is equivalent to a position resolution of 3.0 mm along the LOR.

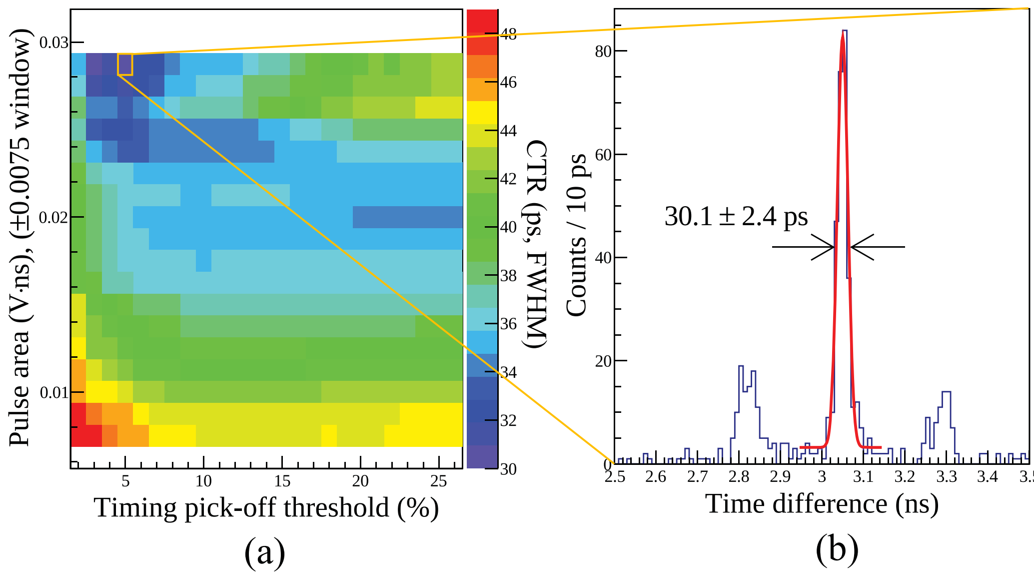

Figure 4. (a) CTRs as functions of the threshold level for timing pick-off and pulse area window. (b) the best CTR histogram obtained by optimizing the threshold level and pulse area window. The CTR was 30.1 $\pm$ 2.4 ps FWHM at 5% threshold with the pulse area window from 0.021 25 to 0.036 25 V ns.

In this study, fully digitized signals were used to obtain the best CTR. However, digitizing all the signals from all the PET detectors is not practical. The timing performance was also evaluated using a conventional analysis method involving leading-edge-discrimination and time walk correction. As a preliminary result, the CTR of 34.0 ps FWHM was obtained.

Although the CTR of 30.1 ps FWHM was obtained, the detection efficiency of γ-rays will not satisfy the requirement of clinical PET detector. The radiator should be replaced by an optimal one, such as PbF_2 with 20 mm thickness, to increase the detection efficiency. Quantitative comparison between the Cherenkov-based and scintillator-based detector is required. In addition, multi-anode readout structure is also required so that the CRI-MCP-PMT is position sensitive. As a technique of multi-channelization is already available in R10754 (Hamamatsu Photonics K. K.), a multi-anode CRI-MCP-PMT can be developed.

5. Conclusions

In this study, we developed the CRI-MCP-PMT to improve the LCE and timing performance. The CTRs were measured and analyzed as functions of the threshold level for timing pick-off and pulse area. The dependence of the CTR on the threshold level and pulse area arises due to the photon counting statistics, which is observed in the case of the scintillation-based detector as well. Consequently, the best CTR of 30.1 $\pm$ 2.4 ps FWHM, which is equivalent to a position resolution of 4.5 $\pm$ 0.3 mm along the LOR, was obtained at 5% threshold for the pulse height with the pulse area window ranging from 0.021 25 to 0.036 25 V ns by using a pair of CRI-MCP-PMTs.

Acknowledgment

The authors appreciate all members who belong to the 43rd department of the Electron Tube Division of Hamamatsu Photonics K. K. for their help in assembling the CRI-MCP-PMTs.

ORCID iDs

R Ota https://orcid.org/0000-0001-6345-1982

References

Ariño-Estrada G *et al* 2018 Towards time-of-flight PET with a semiconductor detector *Phys. Med. Biol.* **63** 04LT01

Berg E *et al* 2015 Optimizing light transport in scintillation crystals for time-of-flight PET: an experimental and optical Monte Carlo simulation study *Biomed. Opt. Express* **6** 2220–30

Brun R and Rademakers F 1997 ROOT-An object oriented data analysis framework *Nucl Instrum. Methods Phys. Res* A **389** 81–6

Brunner S E *et al* 2014 Studies on the Cherenkov effect for improved time resolution of TOF-PET *Trans. Nucl. Sci.* **61** 443–7

Brunner S E *et al* 2017 BGO as a hybrid scintillator/Cherenkov radiator for cost-effective time-of-flight PET *Phys. Med. Biol.* **62** 4421–39

Cates J W and Levin C S 2016 Advances in coincidence time resolution for PET *Phys. Med. Biol.* **61** 2255–64

Cates J W and Levin C S 2018 Evaluation of a clinical TOF-PET detector design that achieves ⩽100 ps coincidence time resolution *Phys. Med. Biol.* **63** 115011

Cates J W *et al* 2015 Analytical calculation of the lower bound on timing resolution for PET scintillation detectors comprising high-aspect-ratio crystal elements *Phys. Med. Biol.* **60** 5141–61

Dolenec R *et al* 2016 The performance of silicon photomultipliers in Cherenkov TOF PET *Trans. Nucl. Sci.* **63** 2478–81

Gundacker S *et al* 2016 Measurement of intrinsic rise times for various L(Y)SO and LuAG scintillators with a general study of prompt photons to achieve 10 ps in TOF-PET *Phys. Med. Biol.* **61** 2802–37

Gundacker S *et al* 2018 Precise rise and decay time measurements of inorganic scintillators by means of x-ray and 511 keV excitation *Nucl. Instrum. Methods Phys. Res.* A **891** 42

Hamamatsu Photonics K. K. 2019 R3809 MCP-PMT datasheet (www.hamamatsu.com/resources/pdf/etd/R3809U-50_TPMH1067E.pdf) (Accessed: 15 January 2019)

Knapitsch A and Lecoq P 2014 Review on photonic crystal coatings for scintillators *Int. J. Mod. Phys.* A **29** 1430070

Korpar S *et al* 2011 Study of TOF PET using Cherenkov light *Nucl. Instrum. Methods Phys. Res.* A **654** 532–8

Kwon S I *et al* 2016 Bismuth germanate coupled to near ultraviolet silicon photomultipliers for time-of-flight PET *Phys. Med. Biol.* **61** L38–47

Lecoq P *et al* 2010 Factors influencing time resolution of scintillators and ways to improve them *Trans. Nucl. Sci.* **57** 2411–6

Lecoq P *et al* 2014 Can transient phenomena help improving time resolution in scintillators? *Trans. Nucl. Sci.* **61** 229–34

Nemallapudi M V *et al* 2015 Sub-100 ps coincidence time resolution for positron emission tomography with LSO:Ce codoped with Ca *Phys. Med. Biol.* **60** 4635–49

Ota R *et al* 2018 Cherenkov radiation-based three-dimensional position-sensitive PET detector: a Monte Carlo study *Med. Phys.* **45** 1999–2008

Ota R *et al* 2019 Timing performance evaluation Cherenkov-based radiation detectors *Nucl. Instrum. Methods Phys. Res.* A **923** 1–4

Schung D *et al* 2015 PET performance and MRI compatibility evaluation of a digital ToF-capable PET/MRI insert equipped with clinical scintillators *Phys. Med. Biol.* **60** 7045–67

Seifert S *et al* 2012 A comprehensive model to predict the timing resolution of SiPM-based scintillation detectors: theory and experimental validation *Trans. Nucl. Sci.* **59** 190–203

Sluis J *et al* 2019 Performance characteristics of the digital biograph vision PET/CT system *J. Nucl. Med.* **60**

Vandenberghe S *et al* 2016 Recent developments in time-of-flight PET *EJNMMI Phys.* **3**